Theor Chim Acta (1986) 69: 475–489

Theoretica Chimica Acta

A Vineyard-type approximation for the distinct term of the dynamic pair correlation function

R. Vogelsang and C. Hoheisel

Theoretische Chemie, Ruhr-Universität Bochum, Universitätsstraße 150, 4630 Bochum, Federal Republic of Germany

(Received September 4, 1985, revised and accepted January 27, 1986)

The distinct term of the van Hove function $G(\boldsymbol{r}, t)$ is approximated by a Vineyard type convolution approximation. The convolution is made with a certain "self" correlation function $G_{sd}(\boldsymbol{r}, t)$ generated by dynamics of pairs of particles. This $G_{sd}(\boldsymbol{r}, t)$ function accounts partly for cross correlation and thus improves the results achievable by the convolution with the pure self term of $G(\boldsymbol{r}, t)$. The results computed by the present method are compared with molecular dynamics data at two liquid-like densities. Good agreement is found for the intermediate range of wave vectors. The approximation is recommended, in particular, for purposes of Fourier transformation.

Key words: van Hove function — Vineyard approximation — Pair-diffusion — Dynamic structure factor — Molecular dynamics

Introduction

The dynamic structure factor $S(\boldsymbol{k}, \omega)$ is the Fourier transform of the van Hove function $G(\boldsymbol{r}, t)$ with respect to space and time. $G(\boldsymbol{r}, t)$ consists of a self term $G_s(\boldsymbol{r}, t)$ which is to a very good approximation represented by a Gauss function and a distinct term $G_d(\boldsymbol{r}, t)$ accessible by molecular dynamics calculations (MDC) for simple fluids. So in principle one can provide the dynamic structure factor on this route via double Fourier inversion of the time dependent pair correlation function $G(\boldsymbol{r}, t)$. However, practically neither the Fourier transformation with respect to space nor that with respect to time can be performed reliably due to the relatively small $(\boldsymbol{r}, t)$ range available by computer simulations according to the smallness of the N-particle system [1]. To remove the problems at least for the space dependence of $G(\boldsymbol{r}, t)$, one could use the Vineyard approximation [2]

for G_d which involves a convolution of G_s with the static pair correlation function $g(r)$. As we restrict our discussion to a simple isotropic liquid in the following, we replace the vector variable dependence of the considered correlation functions by the dependence on the separation only. The static pair correlation function $g(r)$ is today easily determinable up to large separations using various, very accurate extension procedures for MD results or perturbational techniques [3, 4, 5]. Consequently the use of the Vineyard convolution would lead to a "long range" $G_d(r, t)$ function and together with a Gaussian $G_s(r, t)$ a reasonable Fourier inversion of $G(r, t)$ would result.

Unfortunately, the Vineyard approximation does not give good results for G_d, as Rahman has shown by MDC [6]. Rahman has empirically found an improved convolution approximation for G_d, but this is not very simple, has not been tested at different thermodynamic states and is physically not plausible [7]. In view of this, we propose a simple convolution approximation which is physically reasonable and can advantageously be used for G_d.

2. The calculations

We have carried out conventional MDC with a 500 particle system at two thermodynamic states using the interaction potential commonly employed to simulate liquid argon [8]. The details of the calculations, the thermodynamic states and the Lennard-Jones (12-6) potential parameters have been summarized in Table 1. For the chosen thermodynamic states, we have determined the following correlation functions with a statistical error of 1%-5%.

(i) Mean square displacement of particles (MSD);
(ii) MSD of pairs of particles (MSDP);
(iii) cross term of the MSDP (CTP);
(iv) static pair correlation function (PCF);
(v) dynamic PCF (distinct term) at 15 time points.

The method of calculating accurately the MSDP and CTP has been discussed at length in [9] and ought not to be reported again.

Numerical values for the MSDP and the CTP are listed in Table 2. Plots of the MSDP are presented in Fig. 1.

Extension of $g(r)$ has been achieved using the Baxter technique which is known to reproduce $g(r)$ at large r within an accuracy of 1% [4].

The Fourier transforms were obtained by the method of "fast Fourier transformation" (FFT) exploiting spline functions.

3. Results for the Vineyard approximation

The MD results for $G_d(r, t)$ obtained by Rahman [6] are not very accurate and exist solely for three points. From the figures displayed in that work, we conclude that the statistical error for G_d amounts to about 10%. So we have recalculated

Table 1

A. Details of the MD computations

Ensemble	NVEp
Integration	Störmer-Verlet
Number of particles	500
Time step	10^{-14} s
Number of time steps for equilibration	2500
Number of time steps for production	4000
Cutoff radius	2.5σ
Starting configurations	liquid like
CPU-time per 100 steps (Cyber 205 vector processor)	4.1 s

B. Thermodynamic states

	State point 1	2
Temperature	107.6 K	95.2 K
Density[a]	1.306 g cm^{-3}	1.356 g cm^{-3}
Pressure	10 M Pa	0.5 M Pa
Potential energy	5.46 kJ mol^{-1}	5.76 kJ mol^{-1}

C. Lennard-Jones (12-6) potential parameters

$\sigma = 0.3405$ nm
ε/k_b [b] $= 119.8$ K

[a] Mass 39.95 a.u.
[b] Boltzmann constant

these correlation functions for 10 different time points covering the range of 1 ps. We show the time-evolution of the first and the second maximum of G_d normalized by $g(r)$ in Fig. 2. This figure also contains the results for the Vineyard approximation given by the following convolution integral:

$$G_d^{\mathrm{VIN}}(\boldsymbol{r}, t) = \int g(\boldsymbol{r}') G_s(\boldsymbol{r} - \boldsymbol{r}', t)\, d\boldsymbol{r}', \tag{1}$$

$g(r)$ being the MD generated PCF and $G_s(r, t)$ *the* self term of the van Hove function. $G_s(r, t)$ was approximated by a Gaussian term [7]:

$$G_s^{\mathrm{GAU}}(r, t) = \left[\frac{2\pi}{3}\langle r_t^2\rangle\right]^{-3/2} \exp\left[\frac{-r^2}{\frac{2}{3}\langle r_t^2\rangle}\right] \tag{2}$$

where $\langle r_t^2\rangle$ denotes the MSD at time t which was also determined by MD.

Comparison of both curves shows clearly the failure of the Vineyard approximation at short times, for which it predicts a too rapid time decay. For larger times, the curves are only shifted with respect to the ordinate indicating that the

Table 2. Numerical values for the MSDP and the CTP

A. MSDP (state point 1)				B. CTP (state point 1)			
$t/10^{-2}$ ps	$\langle s^2\rangle/\text{Å}^2$	$t/10^{-2}$ ps	$\langle s^2\rangle/\text{Å}^2$	$t/10^{-2}$ ps	$\langle s^2\rangle/\text{Å}^2$	$t/10^{-2}$ ps	$\langle s^2\rangle/\text{Å}^2$
5	0.0	10	0.17	5	0.0	10	0.0
15	0.33	20	0.51	15	0.0	20	0.0
25	0.71	30	0.91	25	0.01	30	0.02
35	1.13	40	1.32	35	0.04	40	0.05
45	1.52	50	1.71	45	0.07	50	0.08
55	1.91	60	2.11	55	0.10	60	0.12
65	2.30	70	2.50	65	0.14	70	0.16
75	2.68	80	2.85	75	0.18	80	0.20
85	3.03	90	3.23	85	0.22	90	0.24
95	3.40	100	3.58	95	0.26	100	0.28
105	3.77	110	3.94	105	0.30	110	0.31
115	4.12	120	4.31	115	0.33	120	0.35
125	4.48	130	4.66	125	0.37	130	0.39
135	4.84	140	5.01	135	0.41	140	0.43
145	5.20	150	5.38	145	0.45	150	0.47
155	5.56	160	5.72	155	0.49	160	0.51
165	5.91	170	6.08	165	0.52	170	0.54
175	6.27	180	6.45	175	0.56	180	0.58
185	6.64	190	6.81	185	0.60	190	0.62
195	7.00	200	7.18	195	0.64	200	0.66
C. MSDP (state point 2)				D. CTP (state point 2)			
5	0.05	10	0.17	5	0.0	10	0.0
15	0.29	20	0.45	15	0.0	20	0.0
25	0.62	30	0.80	25	0.01	30	0.02
35	1.00	40	1.17	35	0.03	40	0.04
45	1.33	50	1.49	45	0.06	50	0.08
55	1.63	60	1.77	55	0.09	60	0.11
65	1.92	70	2.07	65	0.12	70	0.12
75	2.21	80	2.35	75	0.15	80	0.17
85	2.48	90	2.62	85	0.19	90	0.20
95	2.76	100	2.90	95	0.22	100	0.24
105	3.03	110	3.16	105	0.25	110	0.27
115	3.29	120	3.42	115	0.28	120	0.30
125	3.55	130	3.68	125	0.31	130	0.33
135	3.81	140	3.95	135	0.35	140	0.36
145	4.09	150	4.23	145	0.37	150	0.39
155	4.38	160	4.51	155	0.41	160	0.42
165	4.64	170	4.77	165	0.43	170	0.45
175	4.89	180	5.02	175	0.46	180	0.48
185	5.17	190	5.32	185	0.49	190	0.51
195	5.45	200	5.57	195	0.52	200	0.54

prediction of the approximation becomes valid for this intermediate time interval. Such a behaviour might be expected, since for longer time the single particle motion is nearly uncorrelated and thus this assumption being implicitly made for the Vineyard approximation holds. The behaviour of the complete $G_d(r, t)$

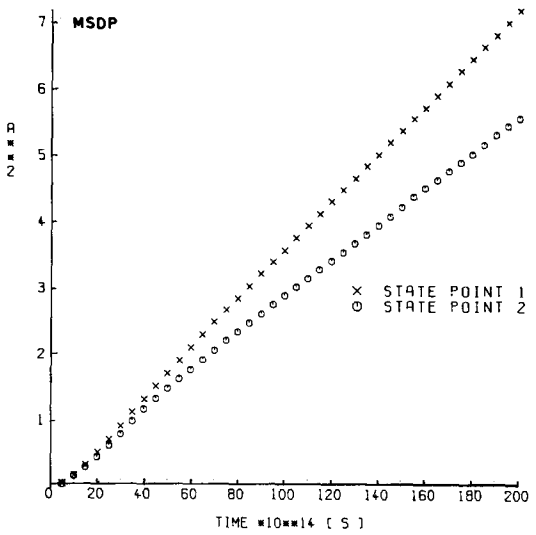

Fig. 1. Mean square displacement of pairs of particles initially in the first coordination shell as a function of time

in the range $0 < r/\sigma < 4.5$ is illustrated for different times in Fig. 3 where additionally the Vineyard convolution is displayed for comparison. We see from the plots that the deviations of the MD generated functions from the Vineyard functions remain also for the larger separations. Later we shall see that the range of large r, i.e., small wave vectors k, cannot correctly be predicted by such an approximation.

4. The present convolution approximation for $G_d(r, t)$

4.1. General considerations and pair diffusion

The results obtained in Sect. 3 indicate that the Vineyard approximation fails to describe the short time behaviour of $G_d(r, t)$ for an intermediate range of separations. The reason for this is naturally the nonseparability of the one particle and the collective motion in a dense system. Both types of motion are governed by the influence of the cage formed by neighbouring particles. This effect has to be accounted for in order to achieve a successful prediction of the "exact" G_d function. An illustrative way of indicating the influence exercised by the "cage"

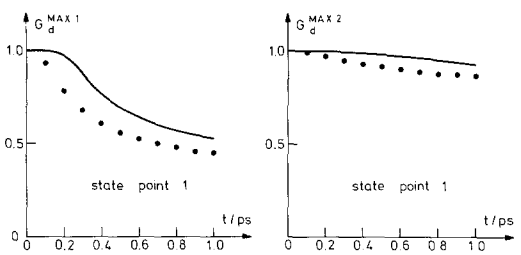

Fig. 2. Height of the first and the second peak of $G_d(r, t)$ as a function of time. The heights are normalized by those of the static pair correlation function $g(r)$. *Lines:* MD; *points:* Vineyard approximation

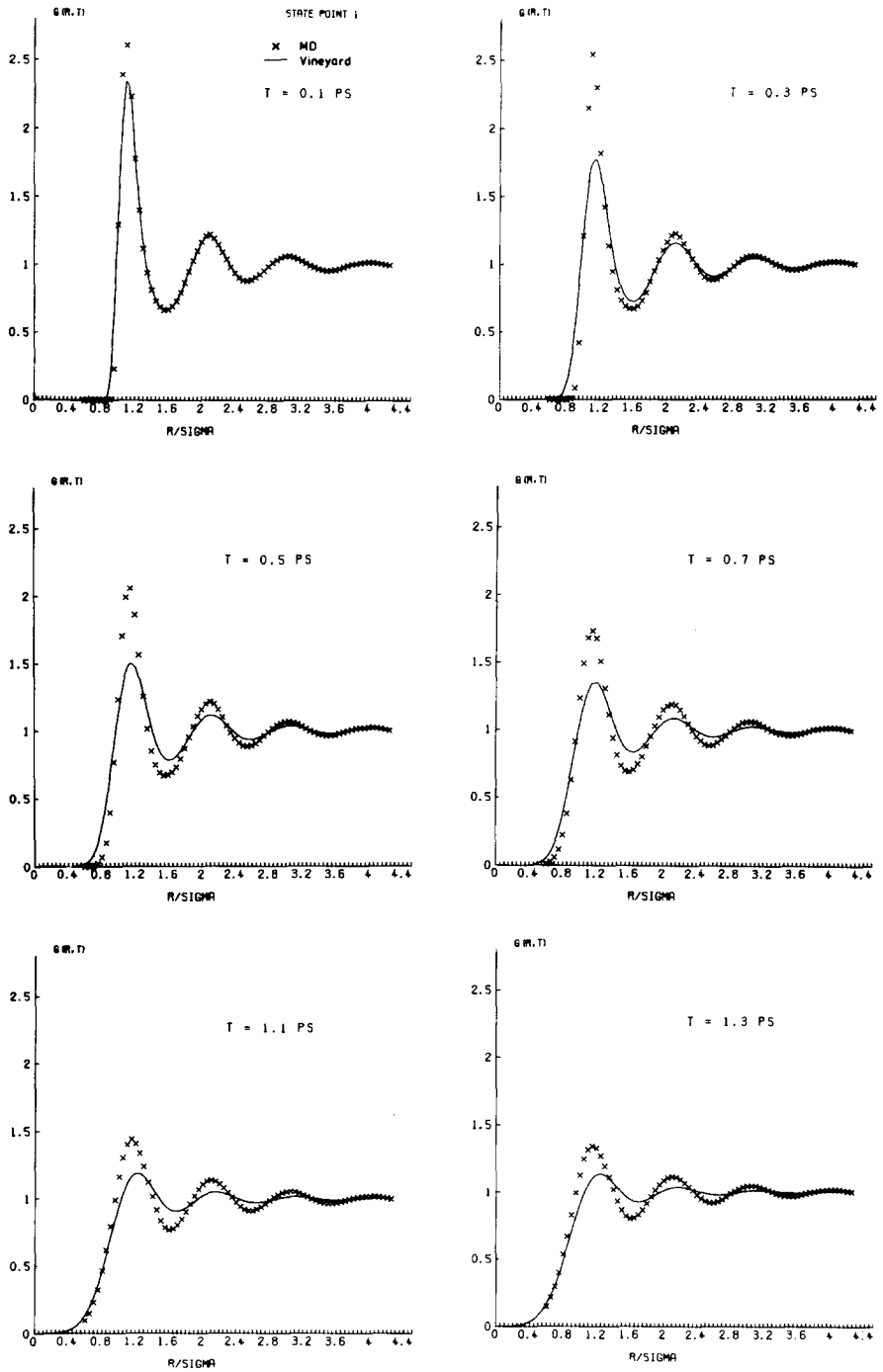

Fig. 3. $G_d(r, t)$ as a function of the separation r for six time points: 0.1 ps, 0.3 ps, 0.5 ps, 0.7 ps, 1.1 ps. 1.3 ps. State point 1. *Lines:* Vineyard approximation; *crosses:* MD

is the computation of the mean square diplacement of single particles and pairs of particles. It suffices here to restrict the discussion to pairs which are initially within the first coordination shell. The results for the motion of pairs of particles [9] may be summarized as follows:

(i) for short times, $0 < t < 0.3$ ps, the MSD and the halved MSDP are not distinguishable;
(ii) significant departures of the MSDP (halved) from the MSD appear after 0.3 ps and persist for long times (>2 ps).

In other words the particle motion at initial times is so strongly localized in the "cage" that cross correlation between pairs or groups of particles vanishes nearly completely. We demonstrate this by Fig. 4 in which the cross term of the MSDP is displayed as a function of time [9]. It is immediately seen that there are no cross contributions for $t < 0.2$ ps and that the CTP is significantly different from 0 for $t > 0.4$ ps We see the connection with the decay of the first peak in G_d plotted in Fig. 2: the decay of the latter in time resembles precisely the growth of the CTP for the initial time period.

The improvement of the convolution approximation is now easy to establish: rather than using the MSD for the Gaussian function in relation (2) we employ the CTP for short times and half the MSDP for long times. For the intermediate region, we have chosen a linear combination of both:

$$G_{sd}^{\mathrm{GAU}}(r, t) = \left(\frac{2\pi}{3}\langle d_t^2\rangle\right)^{-3/2} \exp\left(\frac{-r^2}{\frac{2}{3}\langle d_t^2\rangle}\right) \tag{3}$$

$$\langle d_t^2\rangle \triangleq \frac{D_s}{D_c}\,\mathrm{CTP} - \frac{D_c}{D_p}\,\mathrm{MSDP} \tag{3a}$$

where D_s denotes the self-diffusion coefficient, D_p denotes the diffusion coefficient

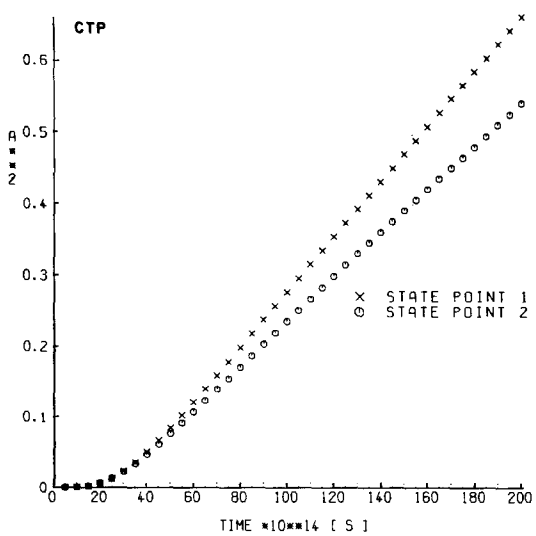

Fig. 4. Cross term of the mean square displacement of pairs of particles as a function of time

Table 3. Self-, pair- and cross-diffusion coefficient for the state points 1 and 2

State point	$D_s \times 10^5/\mathrm{cm}^2\,\mathrm{s}^{-1}$	$D_p \times 10^5/\mathrm{cm}^2\,\mathrm{s}^{-1}$	$D_c \times 10^5/\mathrm{cm}^2\,\mathrm{s}^{-1}$	$(D_s - \frac{1}{2}D_p) \times 10^5/\mathrm{cm}^2\,\mathrm{s}^{-1}$
1	3.51[a] (3.47)[b]	6.01 (6.0)	0.64 (0.52)	0.51 (0.47)
2	2.65 (2.50)	4.51 (4.35)	0.51 (0.42)	0.40 (0.33)

[a] From the present calculations determined by the mean square displacements at larger times
[b] Values in parentheses from [9] determined by the corresponding mean square displacements at larger times and the time integral over the velocity correlation functions

of pairs and D_c denotes the cross-diffusion coefficient. The values for D_s, D_p and D_c have been determined by the corresponding mean square displacements at large times and by the time integral over the velocity correlation functions [9]. These values are tabulated for both states in Table 3. Note that $\langle d_i^2 \rangle$ in Eq. (3a) behaves similarly as the CTP for short times and exactly like half the MSDP for large time. For short times the weighting quotients, D_s/D_c and D_c/D_p, ensure that the right hand side terms of Eq. (3a) are of the same order of magnitude. We have made this difference equal to zero when unphysical, negative values occurred. However, for larger times, where all the three mean square displacements are of linear form, the slope of $\langle d_i^2 \rangle$ equals $6 \cdot (D_s - D_c)$ which is by definition equal to $3D_p$ [9] as it should.

4.2. Results for $G_d(r, t)$

The convolution approximation based on relation (3) is compared with the machine results for the first maximum of G_d at the given states in Figs. 5 and 6. It is clear from these figures that the approximation holds equally well for both thermodynamic states. The comparison of the full G_d-curves in the range $0 < r/\sigma < 4.5$ can be made for state 1 in Fig. 7, where $G_d(r, t)$ and the approximation have been plotted for 6 different time points. Small deviations become apparent for shorter times, but this is expected for reasons which will be discussed in Sect. 5. Our convolution approximation describes the machine results much better than the Vineyard approximation which is illustrated in Fig. 8, where both convolutions are compared with the MD functions for two very different times. So we might

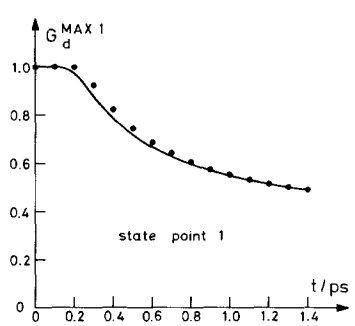

Fig. 5. As in Fig. 2, but the points are the results of the present convolution approximation. State point 1

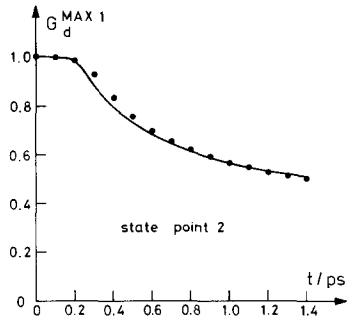

Fig. 6. As in Fig. 5, but for state point 2

expect that the Fourier transform and finally the dynamic structure factor obtained by this method is in good agreement with direct MD results.

4.3. Comparison of the dynamic structure factor computed via the present approximation and by inversion of the directly evaluated intermediate scattering function

To test furthermore our present convolution against direct MD data, we have computed the dynamic structure factor $S(k, \omega)$ for a few k-values larger than $4\sigma^{-1}$. For illustration of the chosen wave vectors, we have plotted the static structure factor $S(k)$ for state 1 obtained by the Baxter method in Fig. 9.

$S(k, \omega)$ was calculated via the following routes:

(i) Evaluation of the static pair correlation function $g(r)$ by MD. Extension of $g(r)$ to large r of about 6σ using the Baxter technique [4]. Calculation of $G_d(r, t)$ by the present convolution for the (r, t) range:

$$0 < r < 6\sigma$$

$$0 < t < 4 \text{ ps}$$

Fourier transformation of G_d with respect to r by FFT. Summation of $\tilde{G}_d(k, t)$ and the Fourier transform of Eq. (2), $\tilde{G}_s^{\text{GAU}}(k, t)$:

$$\tilde{G}_s^{\text{GAU}}(k, t) = \exp(-\tfrac{1}{6}k^2\langle r_t^2\rangle)$$

for the chosen k-values. Fourier inversion of this time correlation function with respect to t yields finally $S(k, \omega)$.

(ii) Direct evaluation of the intermediate scattering function $F(k, t)$ for these k-values by MD [10]. Fourier transformation of $F(k, t)$ with respect to time then gives immediately $S(k, \omega)$.

$S(k, \omega)$ determined by these two methods is plotted as a function of the frequency for four k-values in Figs. 10 and 11. The agreement is very good in all cases showing that our convolution approximation is suitable for such inversion procedures, at least for k-values larger than $4\sigma^{-1}$.

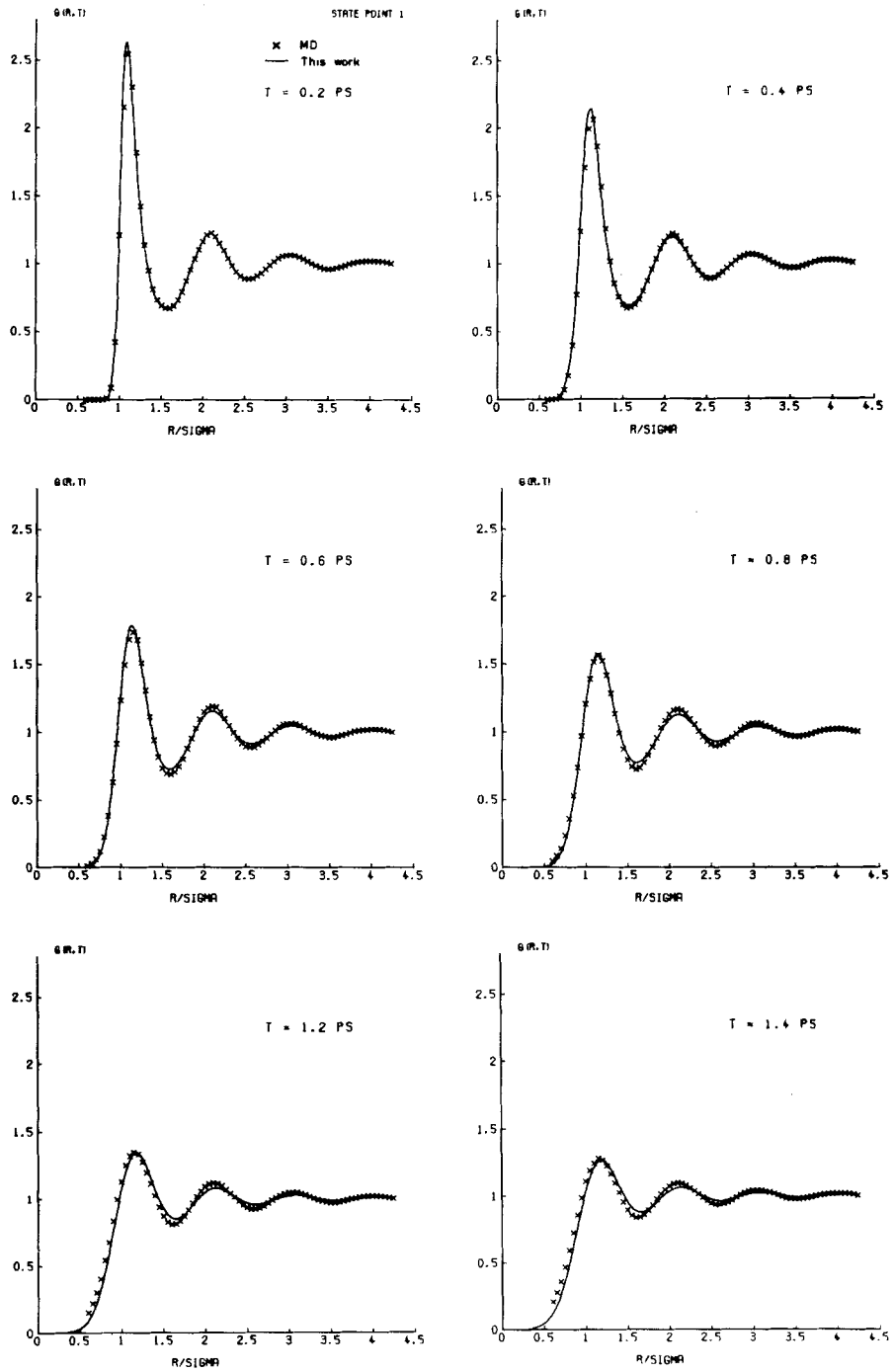

Fig. 7. $G_d(r, t)$ as a function of r for six time points: 0.2 ps, 0.4 ps, 0.6 ps, 0.8 ps, 1.2 ps, 1.4 ps. State point 1. *Lines:* present convolution approximation; *crosses:* MD

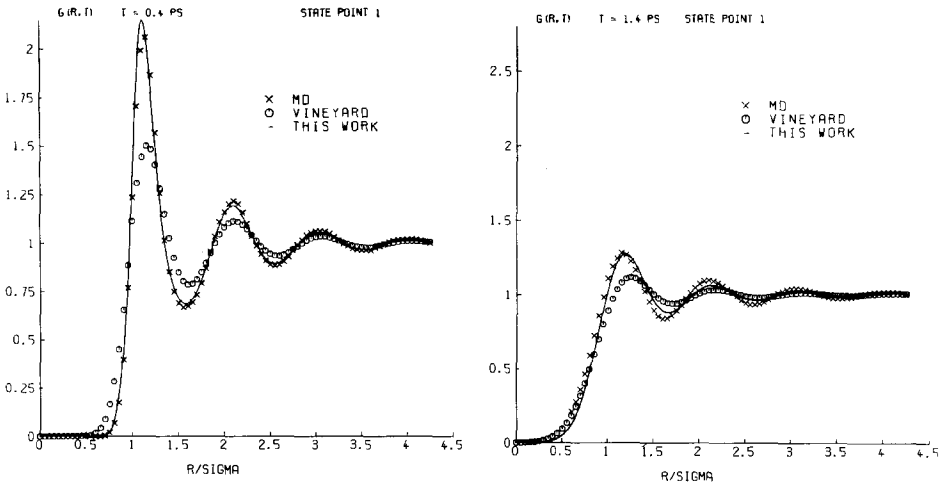

Fig. 8. $G_d(r, t)$ as a function of r for the time points 0.4 ps and 1.4 ps. *Lines:* present approximation; *circles:* Vineyard approximation; *crosses:* MD. State point 1

5. Discussion and conclusion

We have proposed a Vineyard type convolution approximation, which predicts the machine results for $G_d(r, t)$ reliably in the range of $0 < r/\sigma < 5$ and $0 < t < 3$ ps for liquid-like densities of a pure fluid. Our approximation is valid in this (r, t) range and should not be used for much larger times and separations. Particularly

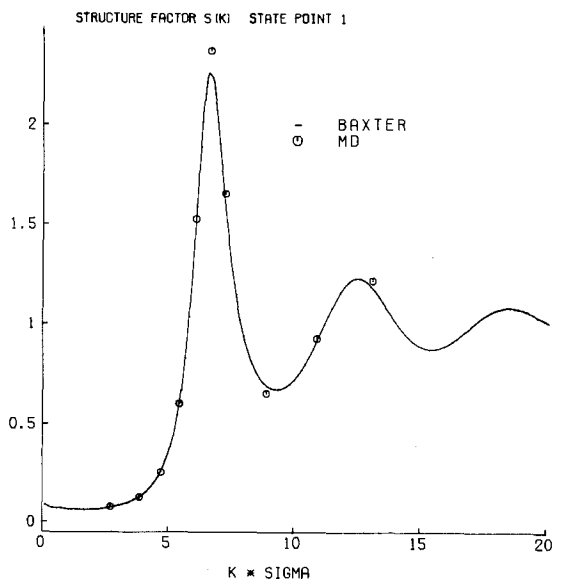

Fig. 9. Static structure factor $S(k)$ for state point 1 calculated by pertubation theory using the Baxter technique

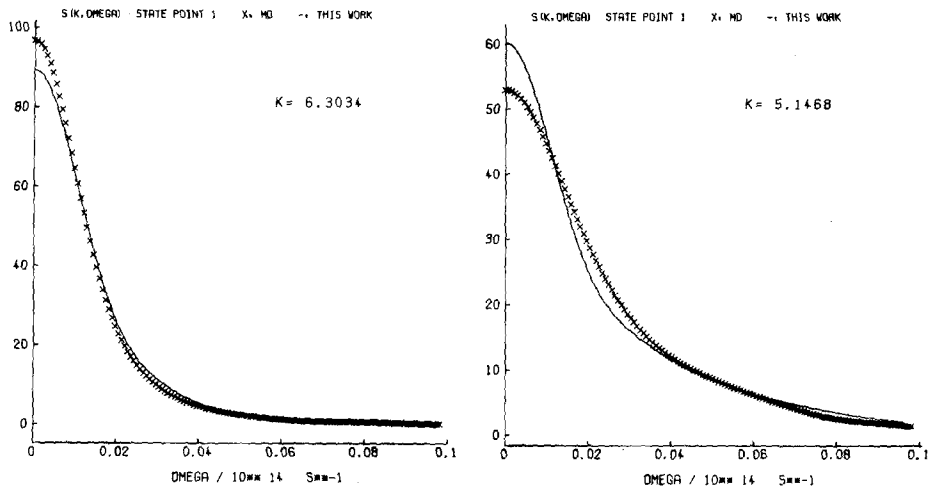

Fig. 10. $S(k, \omega)$ as a function of the frequency for two wave vectors of the amount 5.15 σ^{-1} and 6.30 σ^{-1}. *Lines:* present approximation; *crosses:* MD. $S(k, \omega)$ in units of 10^{-14} s. State point 1

in the hydrodynamic region, this type of convolution cannot lead to reasonable results, as the hydrodynamic behaviour of $S(k, \omega)$ and $S_s(k, \omega)$ is completely different ([2], pp. 226, 238).

We emphasize, however, that the computations required for the present approximation are negligibly small compared with those necessary for a direct determination of $S(k, \omega)$ or $G_d(r, t)$. The CTP and the MSDP can be evaluated with small particle numbers of 108 and 256, and these calculations are of the same kind as those of a mean square displacement of single particles. Moreover, when the data of the CTP given in Table 2 are used, no computations at all have to be

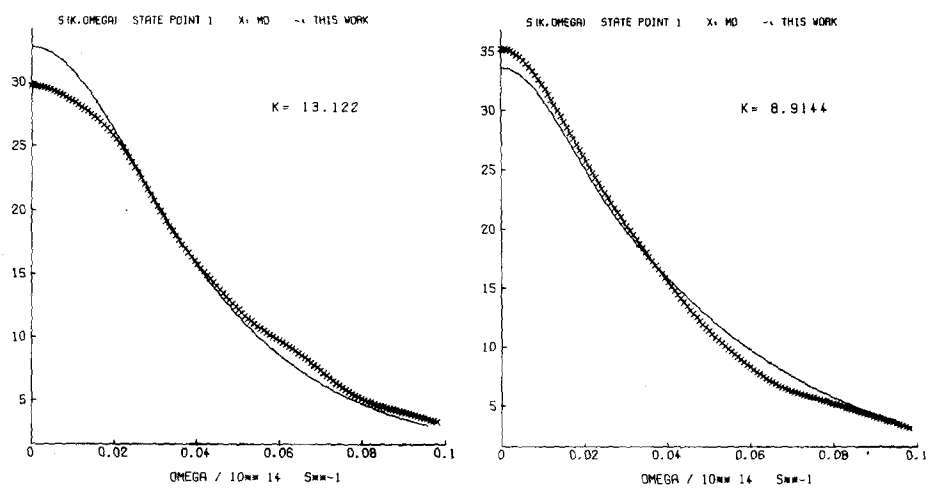

Fig. 11. As in Fig. 10 but for $k = 8.91\ \sigma^{-1}$ and $k = 13.12\ \sigma^{-1}$

performed to evaluate $\langle d_t^2 \rangle$ (Eq. 3a). The short time form of the CTP is nearly identical for the considered thermodynamic states, although the self-diffusion coefficients differ appreciably. So we may use these data for the whole liquid range of Lennard-Jones (LJ) systems. Note that in Eq. (3a) only the short-time behaviour of the CTP is exploited. For larger times, the MSDP determines the time behaviour of Eq. (3a). As the latter is essentially linear, we need only the slope of that function (compare Fig. 1). This slope is given by the pair diffusion coefficient, D_p, of which the half value is to a good approximation 15% smaller than the self-diffusion coefficient (compare Table 3 and [9]).

The self-diffusion coefficient of an LJ system has been determined by Heyes [11] over a larger region of states. Finally, the cross diffusion coefficient can be obtained by the difference between the singlet and the halved pair diffusion coefficient (compare Table 3, last column). So without any new computations the desired mean square displacement, $\langle d_t^2 \rangle$, of Eq. (3a) is available and together with a perturbation approach for $g(r)$ - which takes little computer time - the dynamic structure can be obtained with sufficient accuracy.

To demonstrate this, we have calculated $S(k, \omega)$ for wave vectors as before and a thermodynamic *state not investigated in this work* using the above described method and the Baxter technique to generate $g(r)$ by perturbation theory [3, 4, 12]. The comparison between these results and the directly computed $S(k, \omega)$ is made in Figs. 12 and 13. Evidently these functions agree within about 10% for the chosen k-values larger than $4\sigma^{-1}$.

In contrast to the Vineyard approximation, our convolution preserves the second moment [13] of $S(k, \omega)$ nearly exactly. We show this by decomposition of the approximated intermediate scattering function $F(k, t)$ into the self- and the

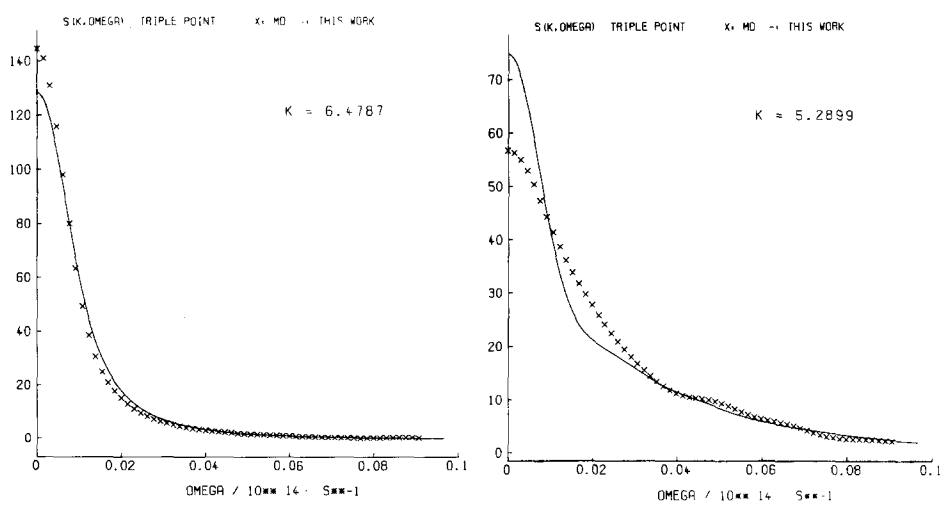

Fig. 12. $S(k, \omega)$ computed directly by MD and by the method proposed in Paragraph 5 using the present convolution and the Baxter theory for $g(r)$. State; 87 K; 1.418 g cm^{-3}. Wave vectors: $k = 5.29\ \sigma^{-1}$, $k = 6.48\ \sigma^{-1}$

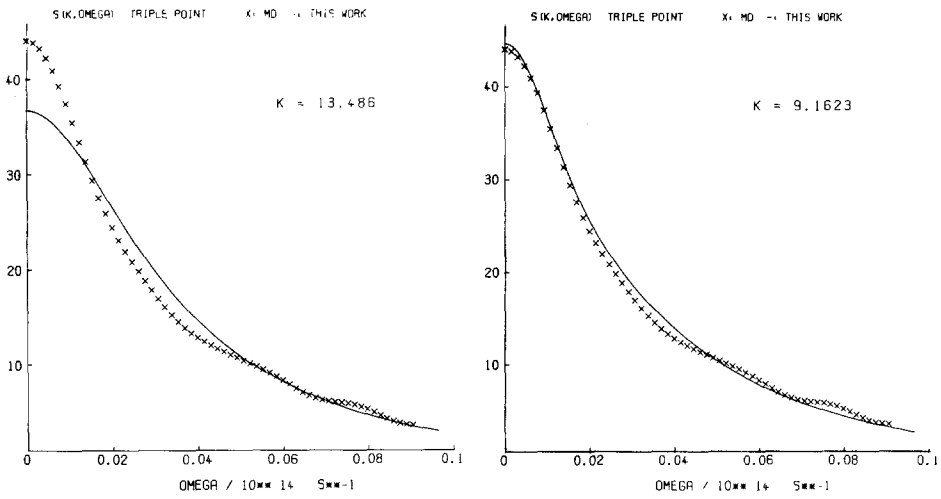

Fig. 13. As in Fig. 12, but for $k = 9.16\,\sigma^{-1}$ and $k = 13.49\,\sigma^{-1}$

distinct term for short times:

$$F(k, t_{\text{short}}) = F_s(k, t_{\text{short}}) + F_{sd}(k, t_{\text{short}})$$
$$= \exp[-\tfrac{1}{6}k^2\langle r_t^2\rangle] + \tilde{g}(k)\exp[-\tfrac{1}{6}k^2\langle d_t^2\rangle]$$
$$= \exp[-\tfrac{1}{6}k^2\langle r_t^2\rangle] + \tilde{g}(k)\exp[-\tfrac{1}{6}k^2(D_s/D_c)\langle c_t^2\rangle]$$

where $\langle c_t^2\rangle$ denotes the CTP and $\tilde{g}(k)$ denotes the Fourier transform of $g(r)$. The MSDP term has been omitted, since the short time behaviour of $\langle d_t^2\rangle$ is essentially determined by $\langle c_t^2\rangle$.

The second derivative of $F(k, t)$ at $t = 0$ yields the second moment of $S(k, \omega)$. Here the second derivative of the first term gives $v_0^2\,k^2$, where v_o is the thermal velocity of a particle, and the second derivative of the second term vanishes completely at $t = 0$, as the cross term of the particle velocities, $\langle \boldsymbol{v}_i^o\ \boldsymbol{v}_j^o\rangle$, is zero by definition [9]. The structure factor approximated by our present convolution has therefore the right second moment, $v_0^2 k^2$. As however the short time behaviour of $G_d(r, t)$ is not exactly reflected by Eq. (3) (see Fig. 6), the higher order moments of $S(k, \omega)$ are surely not given exactly by our approximation.

To include correctly these higher moments (fourth, sixth, ...) of $S(k, \omega)$ one should use a memory function representation of the Fourier components of the local densities $\rho_s(k, t)$ and $\rho_d(k, t)$ [14]. This formal method gives results in good agreement with MD simulations for intermediate and larger wave vectors. However, such calculations are more complicated than the present one. They are not suitable to generate extended $G_d(r, t)$ curves and do not allow a proper physical insight into the dynamical process (compare [15]).

Our study is based on the assumption that the Gaussian model for $G_{sd}(r, t)$ works well for the considered time period. This is not true for a certain intermediate time interval, where $G_s(r, t)$ shows non-Gaussian behaviour [13]. Part of the

discrepancies between the calculated $S(k, \omega)$ and the MD generated one originates presumably from the use of the Gaussian form for $G_s(r, t)$ and $G_{sd}(r, t)$. A straightforward computation of these functions by MD could throw more light on this. We plan to do calculations of this kind in a later study.

Acknowledgements. We are grateful to the 'Rechenzentrum Bochum' (for computing time on the CYBER 205), D. Runzer (for diagrams), D. Hiltscher (for photography) and to S. Lange (for typing). We furthermore thank the Deutsche Forschungsgemeinschaft for financial support (HO 626/6-1, 6-2). We thank a referee for critical and helpful comments on our manuscript.

References

1. Rowlinson JS, Evans M (1976) Ann Rep Prog Chem, Sect A; Phys Inorg Chem 5
2. Hansen JP, McDonald IR (1976) Theory of simple liquids. Academic Press, New York
3. Baxter R J (1970) J Chem Phys 52:4559
4. Vogelsang R, Hoheisel C (1985) Molec Phys 55:1339
5. Weeks JD, Chandler D, Andersen HC (1971) J Chem Phys 54:5237
6. Rahman A (1964) Phys Rev A 136:405
7. Berne BJ (1971) In: Eyring H, Henderson D, Jost W (eds) Physical Chemistry. An advanced treatise vol VIII B. Academic Press, New York
8. Vesely F (1978) Computerexperimnete an Flüssigkeitsmodellen. Physik Verlag, Weinheim
9. Hoheisel C, Zeidler MD (1985) Molec Phys 54:1275
10. Schoen M, Vogelsang R, Hoheisel C (1986) Molec Phys 57:445
11. Heyes D M (1983) J Chem Soc Faraday Trans 2 79:1741
12. Baxter R J (1971) In: Eyring H, Henderson D, Jost W (eds) Physical Chemistry. An advanced treatise vol VIII A. Academic Press, New York
13. Boon JP, Yip S (1980) Molecular hydrodynamics. McGraw-Hill, New York
14. Kim K, Nelkin M (1971) Phys Rev A4:2065
15. Lucas K, Moser B (1979) Molec Phys 37:1849